Make carriers
→Charge transfer

Make conduction path

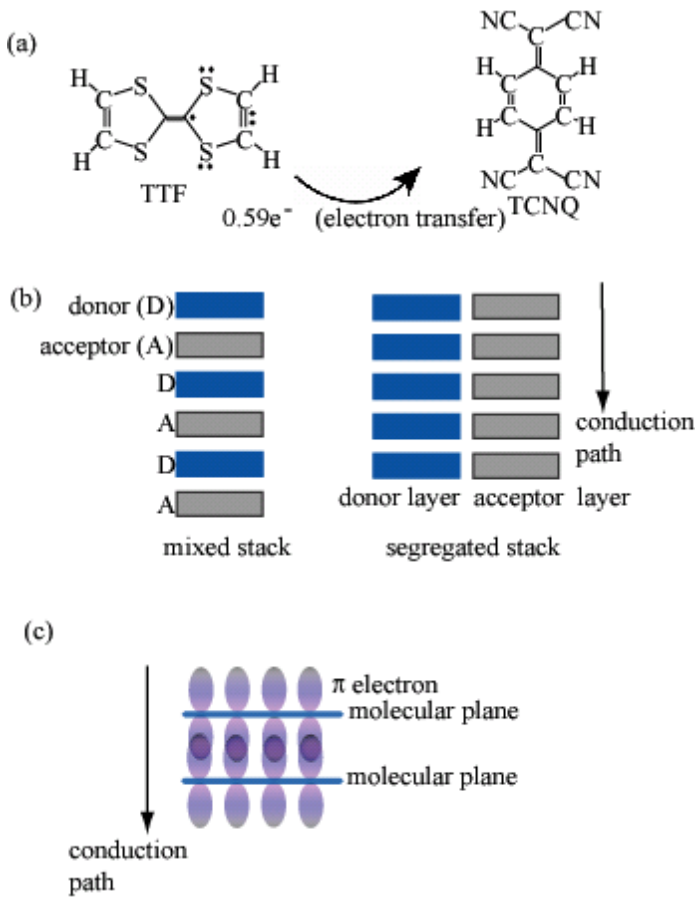

Fig. 9.1 (a) Charge transfer from an organic donor of TTF (tetrathiafulvalene) to an acceptor of TCNQ (tetracyanoquinodimethane) by $0.59e^-$, (b) mixed stack and segregated stack, and (c) a stack of π electron molecular plane.

Fig. 9.2 Molecular structures of donors and acceptors constituting organic superconductors and related materials.

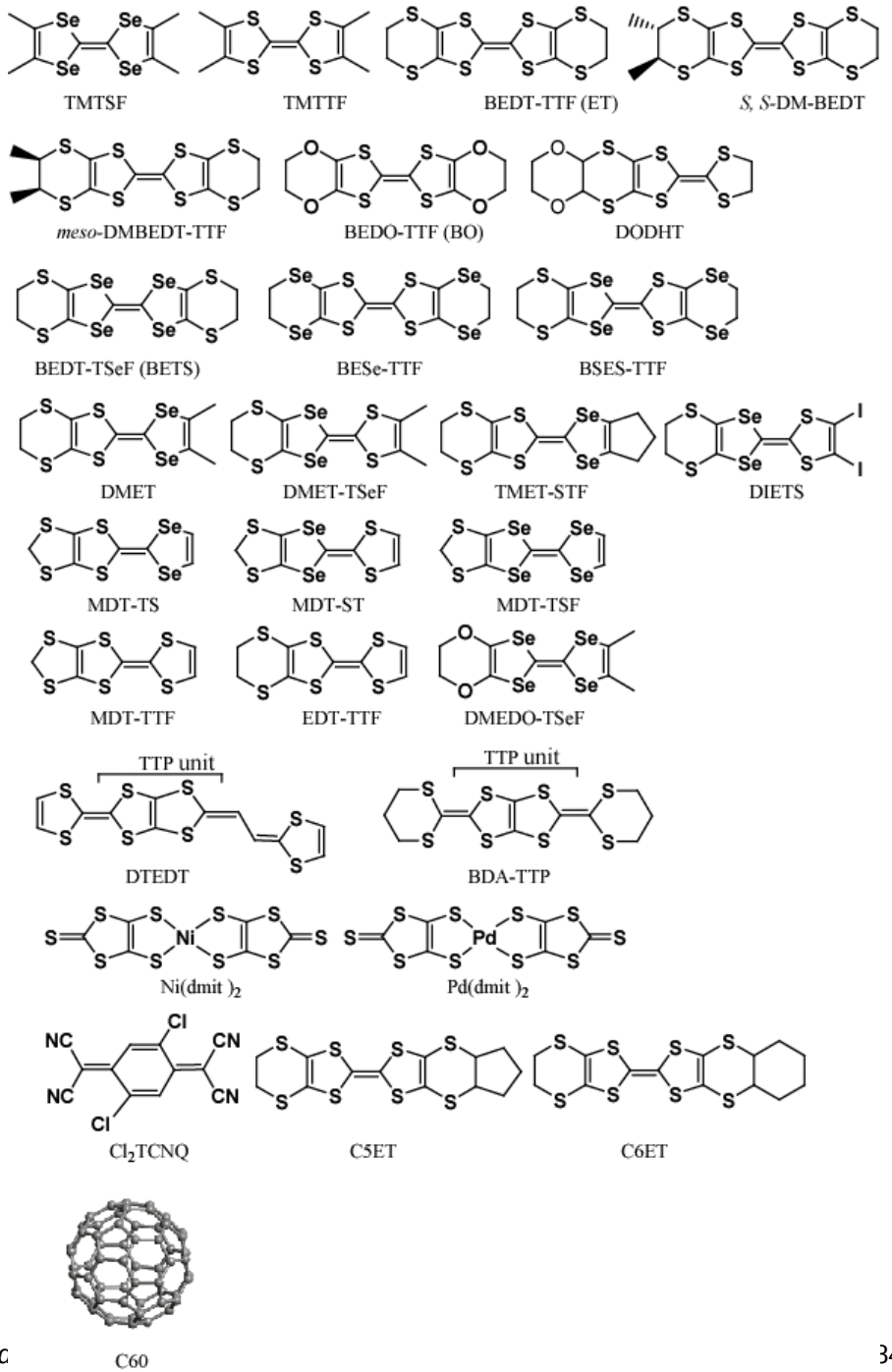

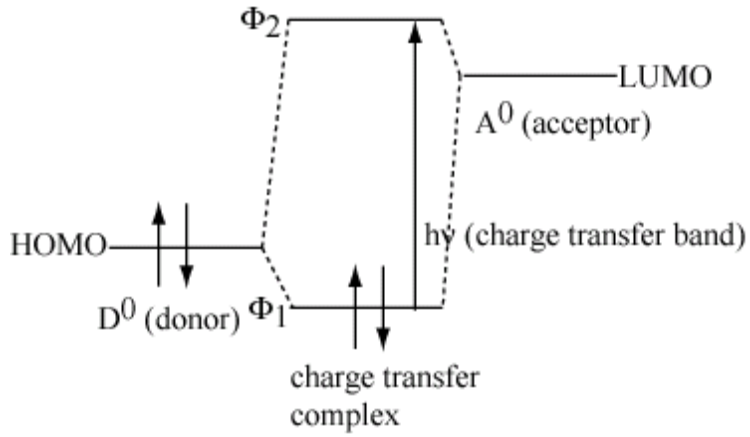

bonding orbital $\Phi_1 = a\ \Phi(D^0A^0) + b\ \Phi(D^+A^-)$

anti-bonding orbital $\Phi_2 = a^*\ \Phi(D^0A^0) - b^*\ \Phi(D^+A^-)$

Fig. 9.3 Charge transfer from HOMO (the highest occupied molecular orbital) to LUMO (the lowest unoccupied molecular orbital) and charge transfer band.

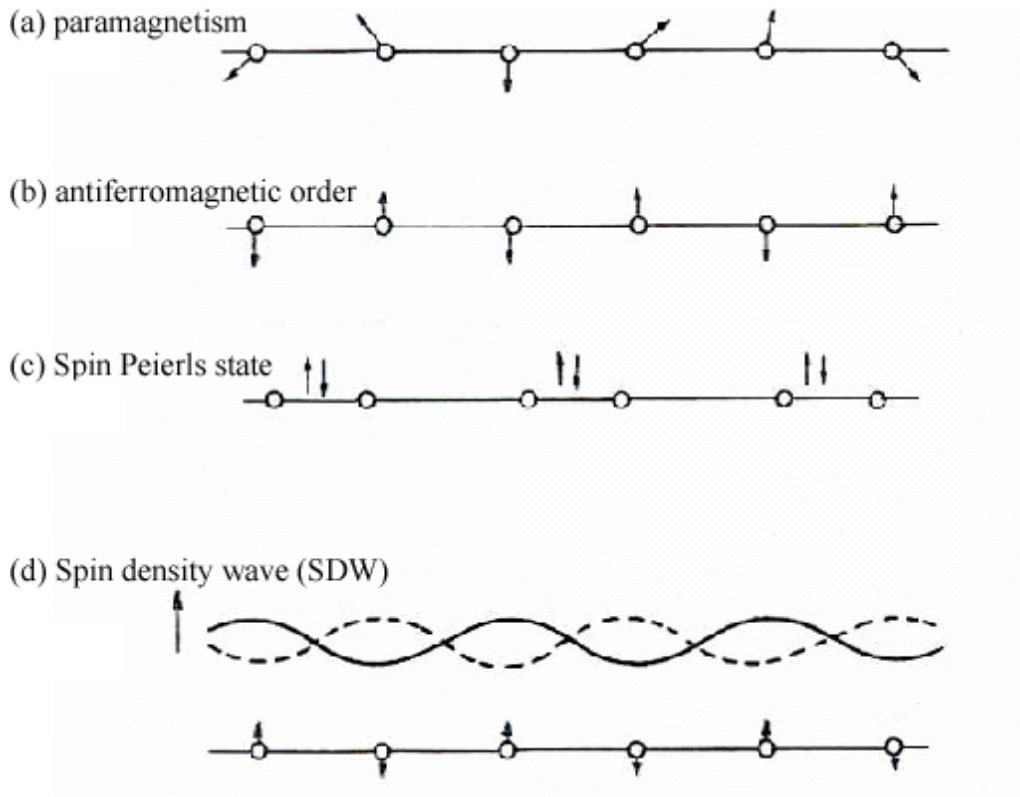

Fig. 9.4 (a) Paramagnetism (PM), (b) antiferromagnetic order (AF), (c) Spin Peierls state (SP), and (d) spin density wave (SDW) state.

Fig. 9.5 (a) Single crystals of κ-(BEDT-TTF)$_2$Cu(NCS)$_2$ and electrocrystallization of (b) 100 ml cell, and (c) 20 ml cell.

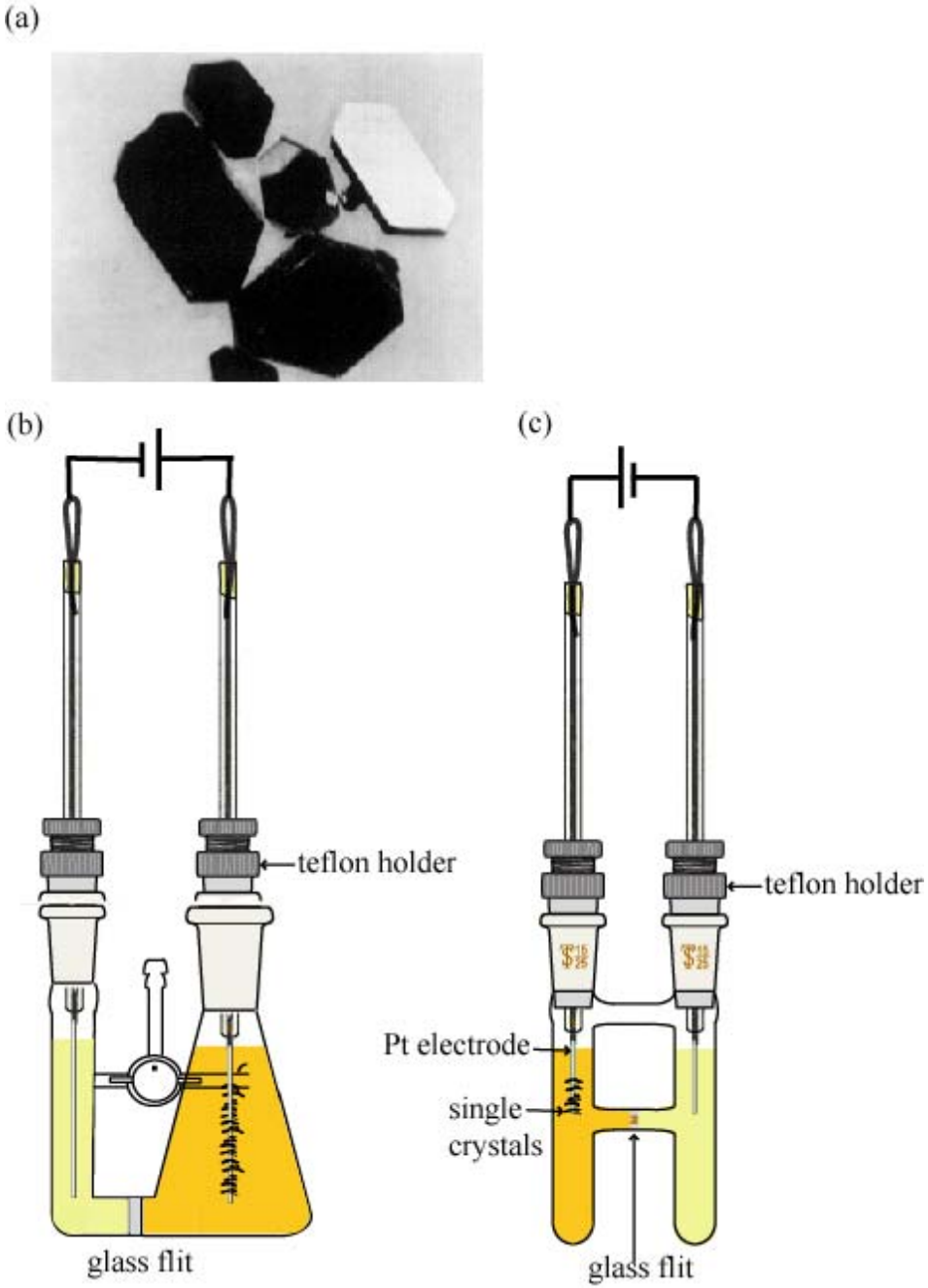

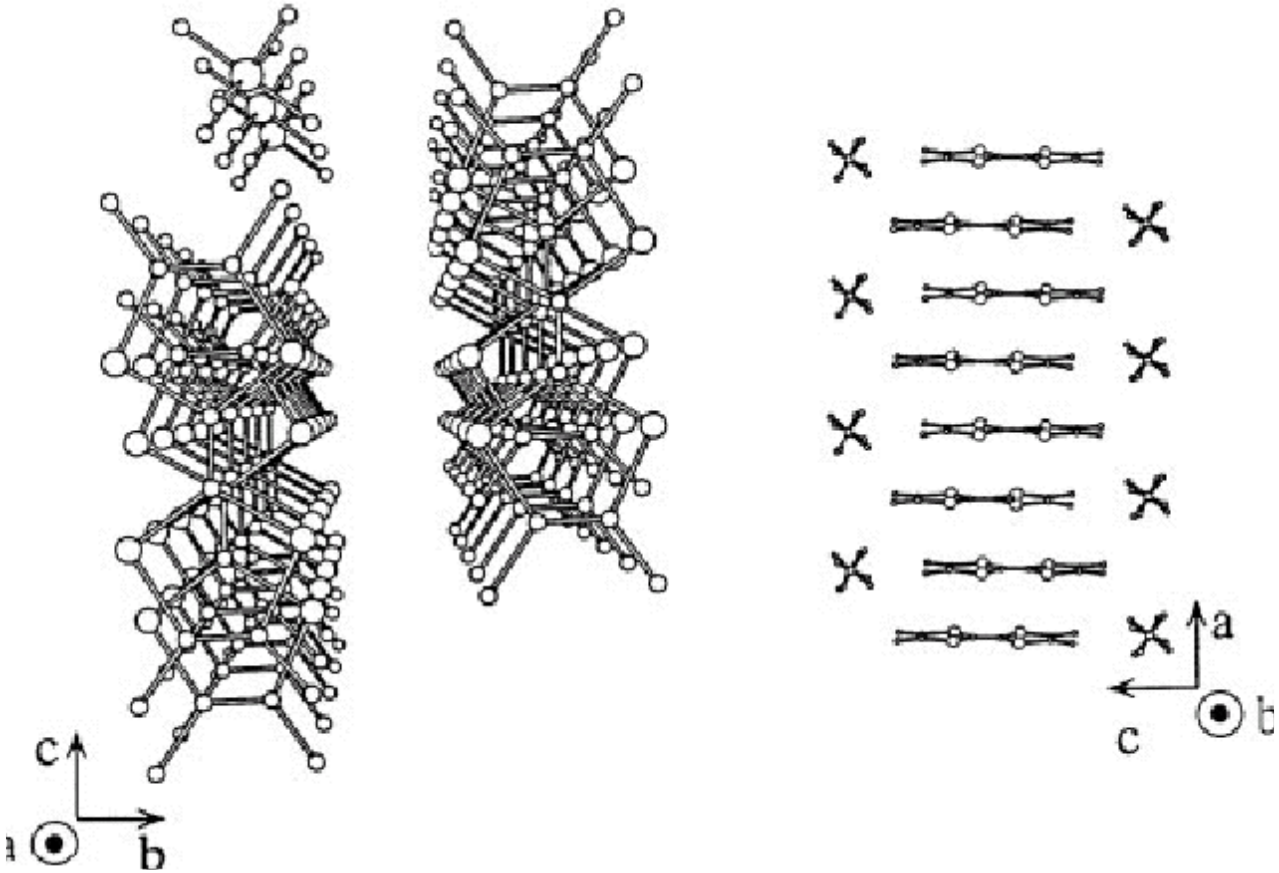

Fig. 9.6 (a) Crystal structure of $TMTSF_2PF_6$

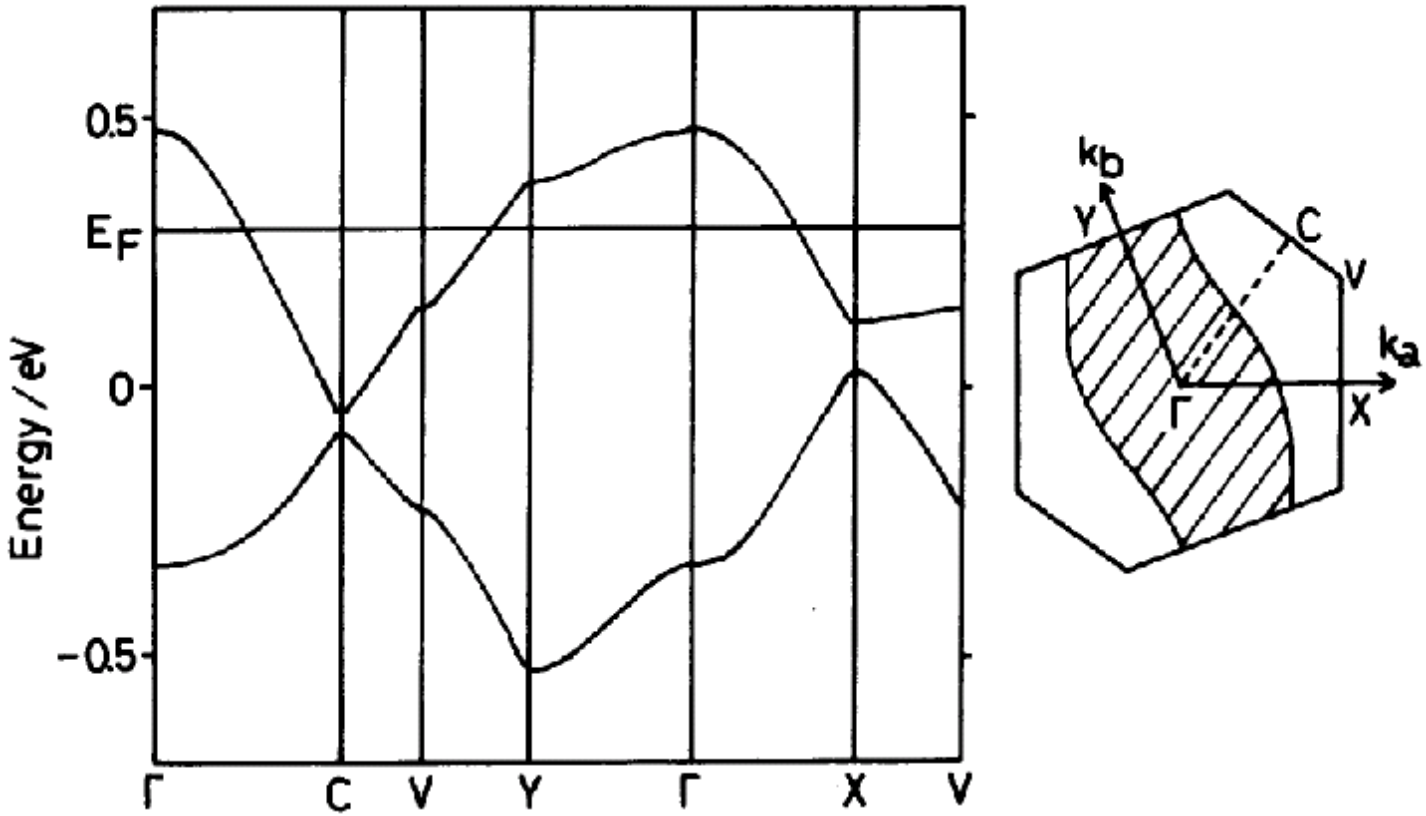

Fig. 9.6 (b) Fermi surface of $TMTSF_2PF_6$.

Fig. 9.6 (c) Metal-insulator transition of $TMTSF_2X$ (X = NO_3, PF_6, AsF_6, and BF_4)

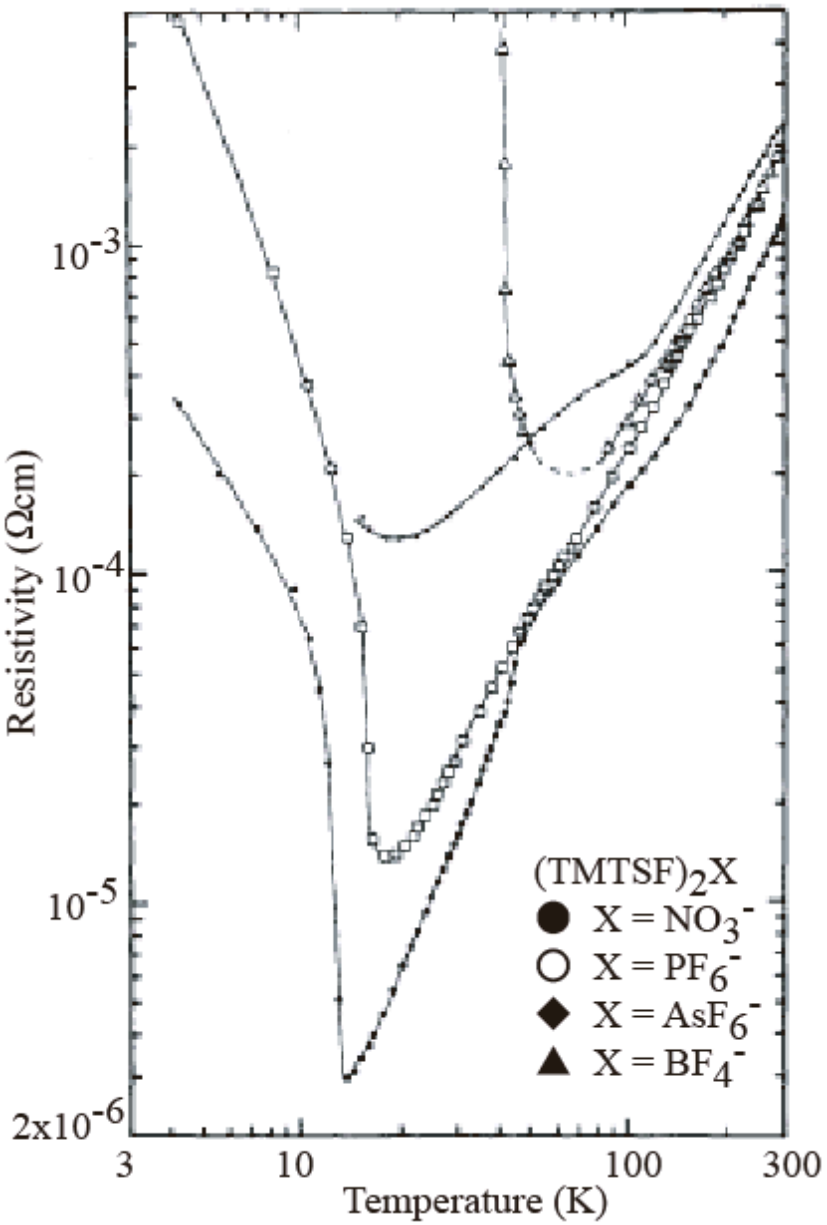

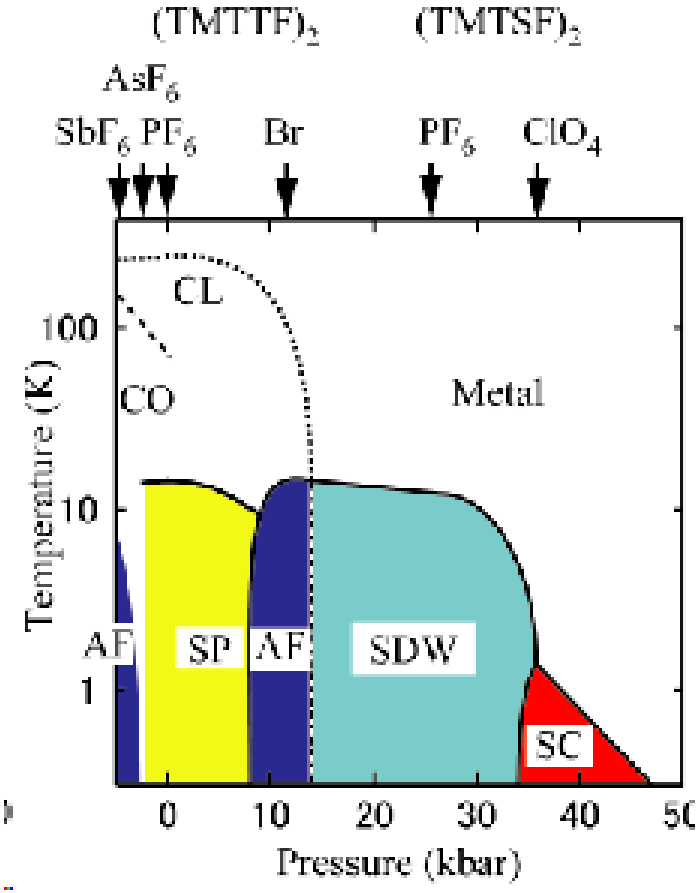

Fig. 9.6(d) Electronic phase diagram of $(TMTTF)_2X$ and $(TMTSF)_2X$.

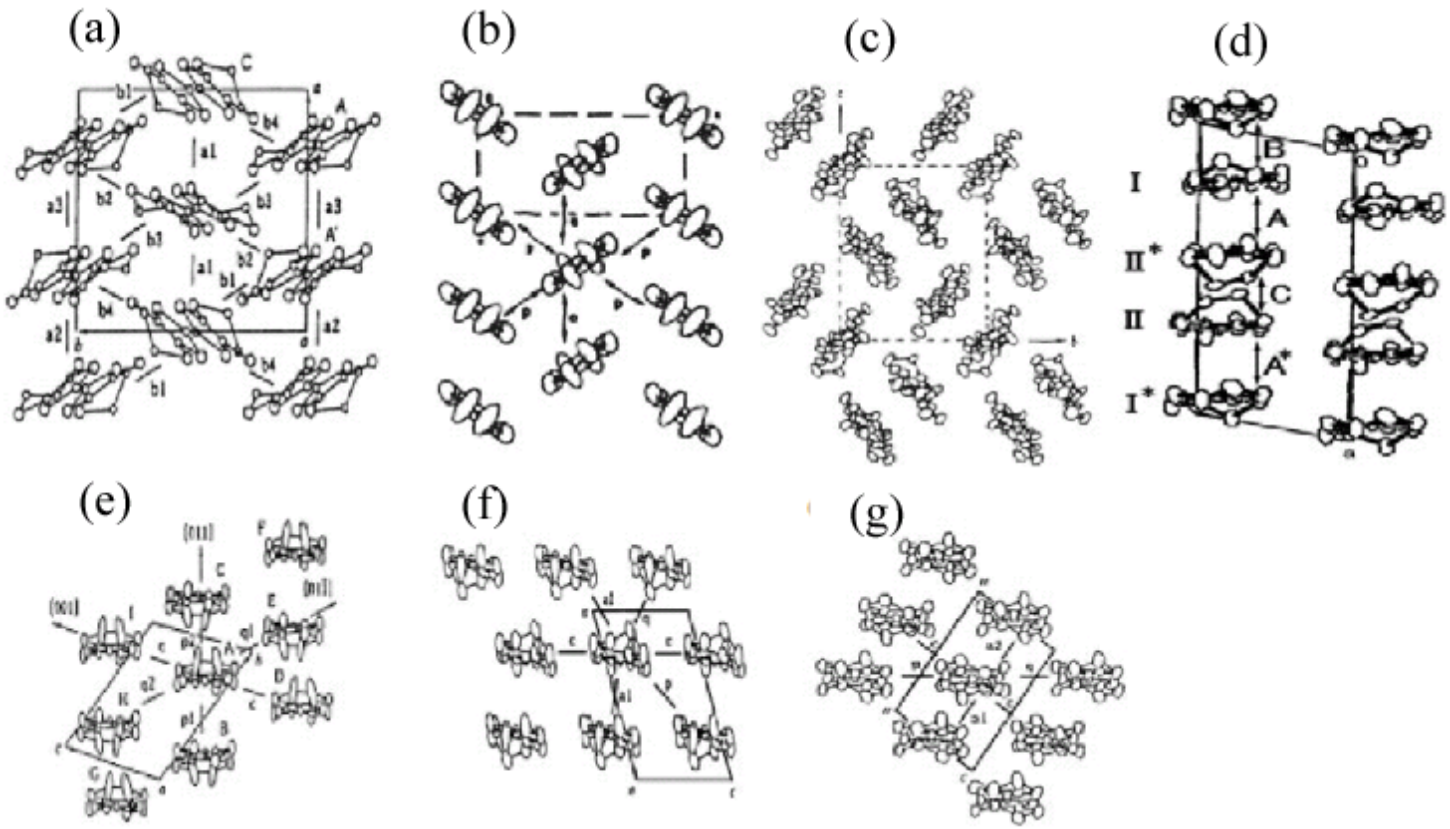

Fig. 9.7 Molecular arrangements of (a) α-type, (b) θ-type, (c) κ-type, (d) λ-type, (e) β-type, (f) β'-type, and (g) β''-type BEDT-TTF salts.

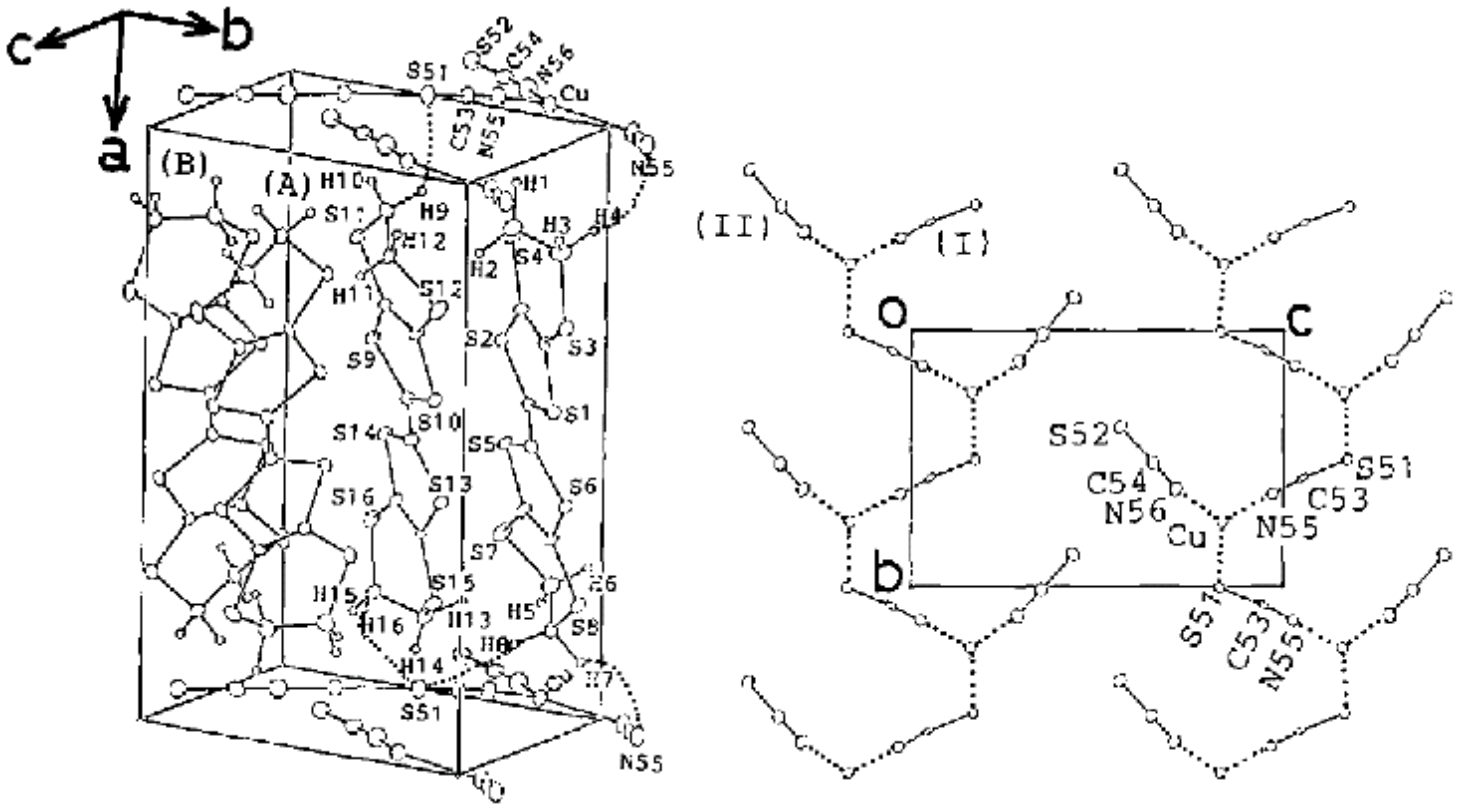

Fig. 9.8 (a) Crystal structure of κ-(BEDT-TTF)$_2$Cu(NCS)$_2$.

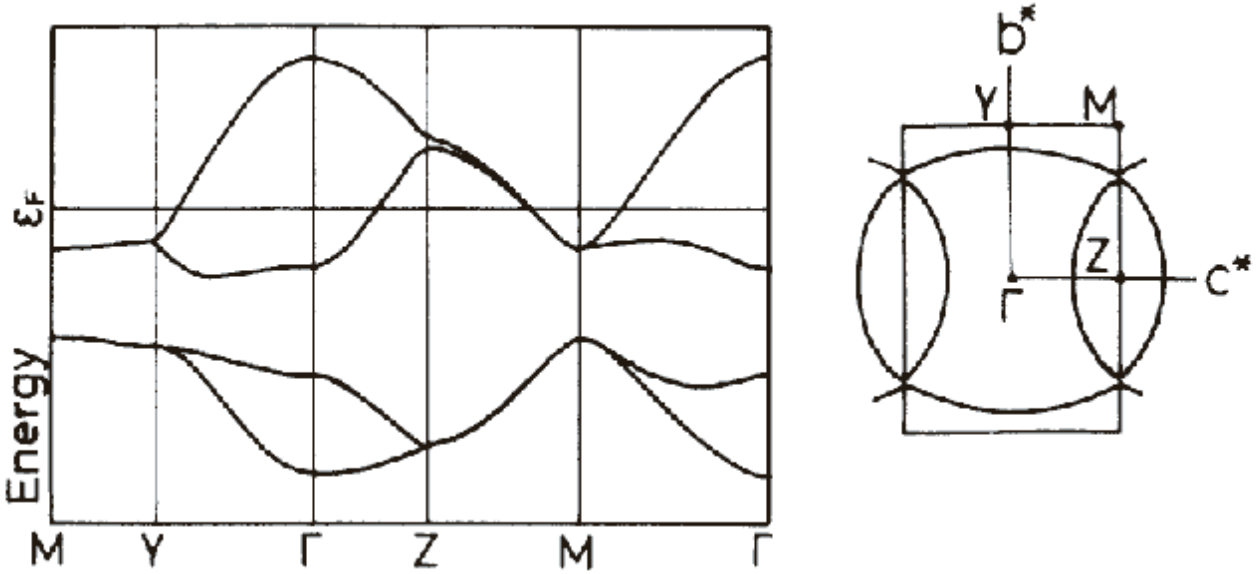

Fig. 9.8 (b) Band structure of κ-(BEDT-TTF)$_2$Cu(NCS)$_2$.

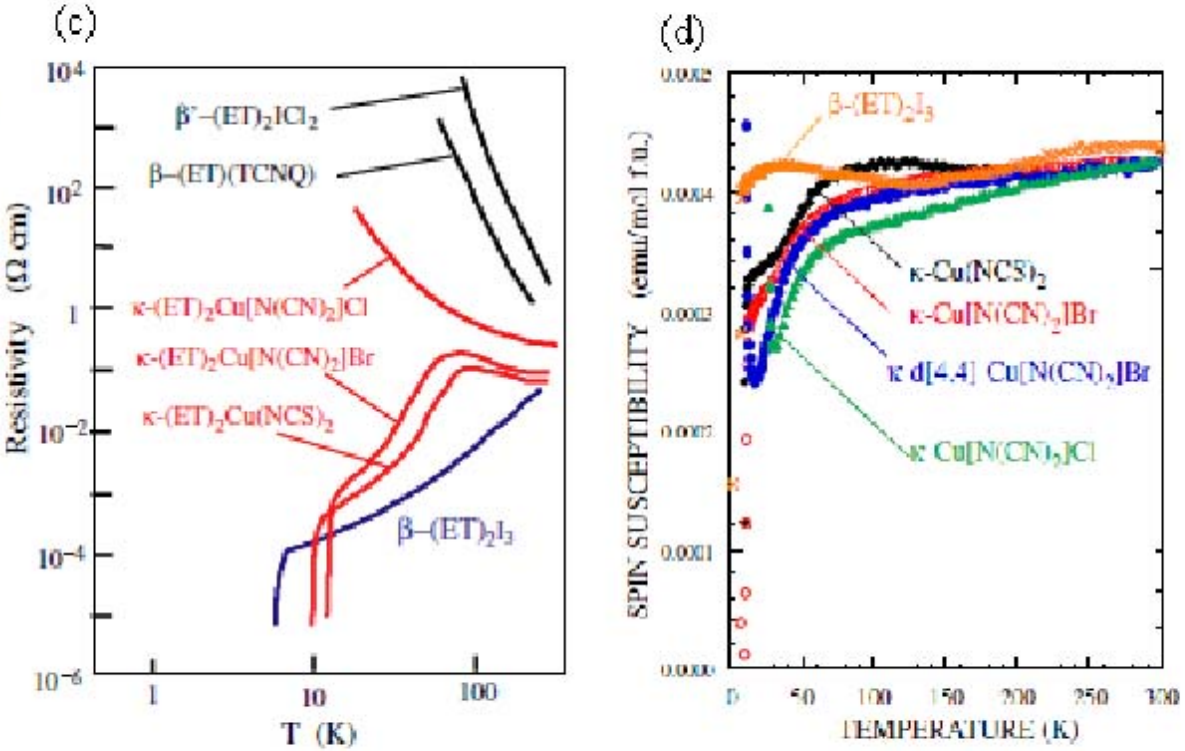

Fig. 9.8 (c) electrical resistivities, and (d) magnetic susceptibilities for a series of κ-type BEDT-TTF salts.

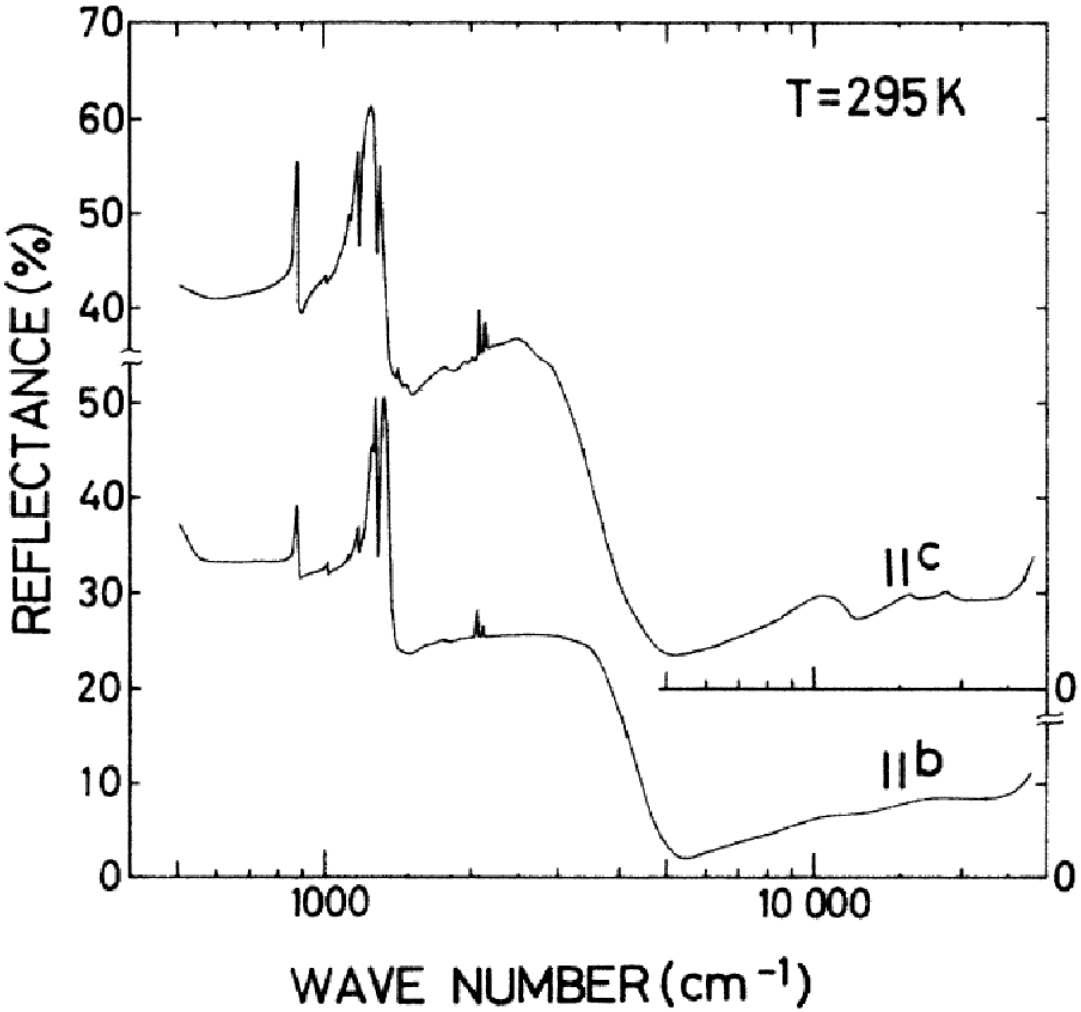

Fig. 9.9 Reflectance spectra of κ-(BEDT-TTF)$_2$Cu(NCS)$_2$.